Invited Paper

Tunable MEMS Fabry-Pérot filters for infrared microspectrometers: A review

Martin Ebermann*[1], Norbert Neumann[1], Karla Hiller[2], Mario Seifert[2], Marco Meinig[3], Steffen Kurth[3]

[1] InfraTec GmbH, Gostritzer Str. 61–63, 01217 Dresden, Germany

[2] Universität Chemnitz, Zentrum für Mikrotechnologien, 09107 Chemnitz, Germany

[3] Fraunhofer ENAS, Technologie-Campus 3, 09126 Chemnitz, Germany

ABSTRACT

Many application fields of infrared spectroscopy require small, robust and transportable spectrometers, which are considerable less costly than existing products. Therefore microspectrometer technologies are rapidly emerging and many research groups spend effort on this. Compared to other kinds of devices, micromachined tunable Fabry-Pérot filters are best suited in terms of miniaturization and optical throughput. This paper gives a review of µFP filters for infrared spectroscopy. Different approaches from several groups are compared. Optical performance parameters like wavelength tuning range, spectral resolution and aperture size as well as complexity of fabrication and costs are discussed.

1. INTRODUCTION

Infrared spectroscopy is a powerful analysis method, because many substances can be distinguished reliably by their unique absorption spectra. Conventional infrared spectrometers are complex and expensive instruments with limited portability because of their size and power consumption. There is a huge variety of applications like medical diagnostics and health care (e.g. sensing gases in the human breath), detection of hazardous substances (e.g. combustible and toxic gases, detection of explosives), process monitoring in the pharmaceutical and chemical industry and a lot more. They all generate a strong demand for small, robust and transportable spectrometers, which are considerable less costly than existing products.

For visible and the near-infrared wavelengths diverse solutions based on gratings and detector arrays were established. However, for the mid and long-wave infrared (3 - 12 µm) they have not been successful for two reasons: limited optical throughput and costly array detectors. Fourier type (FT) spectrometers (e.g. Michelson interferometers) on the other hand are difficult to implement in MEMS technology due to their complex optical setup. There are some approaches for MEMS FT systems that can be found in literature and even commercialized products. But once more, they mainly suffer from a limited optical throughput. A comprehensive review of different infrared microspectrometer technologies was given by R. A. Crocombe in 2008.[1–4] In comparison to the aforementioned classical concepts, micromachined Fabry-Pérot interferometers (FPI) used as tunable filters (µFP filters, µFPF) seem to be most suitable. The arrangement of two parallel reflectors in a very short distance forming the FP cavity can be implemented quite easily with MEMS technology which allows for a high degree of miniaturization, while at the same time maintaining a sufficiently large throughput.

The present paper is a review of the current µFP filter technology reported in the literature, in particular for infrared wavelengths. It is limited to filters that are based on air-gap tuning, since alternative approaches like angle or index tuning have serious drawbacks. Furthermore it mainly focuses on single point detection systems, which can be used for gas sensing or similar applications. However, some side trips to neighboring applications like hyperspectral imaging or the visible spectral range are made for the sake of completeness. Several papers of different research groups reviewing there own technology have been published already.[5,6] Here a comparison of the different technological approaches shall be provided. It includes monolithically surface micromachined filters with free standing reflector membranes made by sacrificial layer etching as well as bulk micromachined filters constructed of bonded wafers. The authors did their best to cover the most relevant developments and apologize for any important that could have been missed.

* m.ebermann@infratec.de; phone +49 351 871 8625; fax +49 351 871 8727; www.infratec.de

MOEMS and Miniaturized Systems XV, edited by Wibool Piyawattanametha, Yong-Hwa Park, Proc. of SPIE Vol. 9760, 97600H · © 2016 SPIE
CCC code: 0277-786X/16/$18 · doi: 10.1117/12.2209288

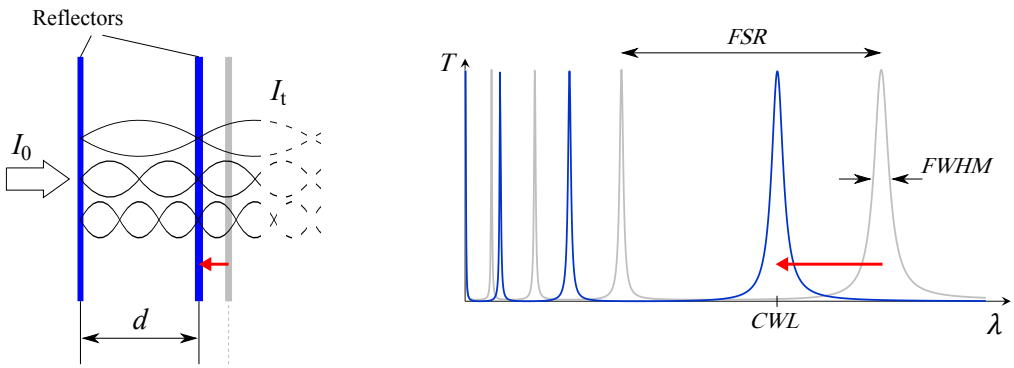

Figure 1. Basic structure and working principle of the FPI. The red arrows should indicate tuning of the peak position (center wavelength *CWL*) by adjusting the reflector spacing *d*.

2. BACKGROUND

After its invention by Charles Fabry and Alfred Pérot more than hundred years ago,[7] the FPI found applications in very sophisticated optical instruments. Maybe the most impressive ones are the spectral sensors of large astronomic telescopes, where it is used up to the present day. However, its basic structure consisting of only two flat, parallel and partially transmissive mirrors makes it a very clear candidate for highly integrated and miniaturized systems. After MEMS technology has been established during the 1980s it was mainly due the telecom boom in the late 90s that optical microsystems (MOEMS) became more and more into focus.[1,2] Nonetheless, to the best of the authors knowledge, the first publication on µFPF dates back to 1987, when Mallinson et. al.[8] presented a device for wavelength division multiplexing (WDM) in the NIR region and it was to take only up the mid 90s, that the first µFPF for spectral sensors showed up.[9,10]

The theoretical background of the FPI can be found in many textbooks[11–13] or in the literature that is referenced within this paper. Here it will suffice to mention just a few design aspects, that are important for its realization in MEMS and the usage as a tunable filter (see also figure 1):

- As a fundamental rule for all kind of spectrometers or spectral sensors, resolution, spectral range and optical throughput (which translates into signal to noise ratio) are always conflicting requierements. They should be carefully balanced for the specificic application. Of course, the size and type of detector, the light source and how all these components are integrated into the whole sensor system play also an very important role.
- An FPI creates a series of transmittance peaks of successive interference orders separated by the free spectral range (*FSR*). For large tuning ranges, a low order has to be selected, which, for the infrared region, results in a resonator length d (mirror spacing) of only a few microns. Operating in higher orders can help to increase the spectral resolution by reducing the peak bandwidth (*FWHM*) but, at the same time, the *FSR* and, consequently the tuning range shrink.
- The Finesse and spectral resolution of a µFPF depend on the reflectance of the mirrors, but also on so called defects like bow, tilt and roughness as well as on the cone angle of the transmitted beam. Usually this results in very tight design constraints.
- Apart from a few exceptions, distributed Bragg reflectors (DBR) made from dielectric quarterwave layers with alternating low (L) and high (H) refractive index are used,[12] which have to be designed and fabricated for the specific spectral range. The materials should exhibit very low absorption and a high refractive index contrast.
- Tuning is achieved by adjusting the resonator length d by means of electrostatic actuation (without any exception for the work referenced in this review). Normally one of the reflector plates is fixed and the other is suspended by springs or a tensioned membrane, that provides the restoring force. The well known pull-in phenomenon induces another design restriction to the tuning range: driven by a constant voltage a parallel plate actuator can be operated in a stable manner only within one third of the initial electrode gap.

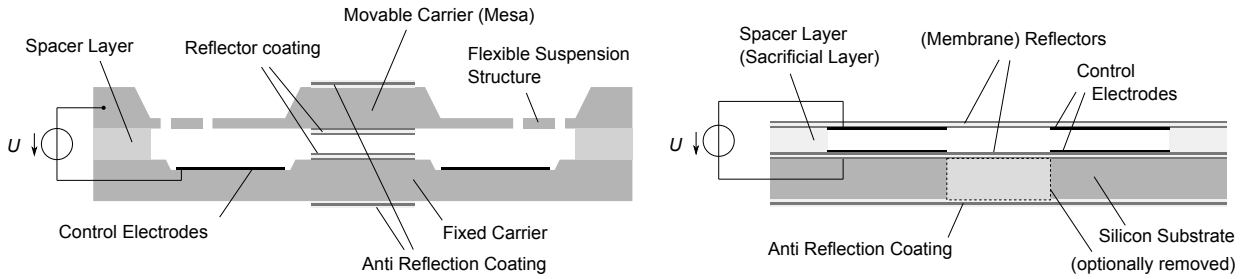

Figure 2. Typical cross sections of µFPF fabricated by means of a) bulk micromachining and wafer bonding, b) surface micromachining and sacrificial layer etching.

Table 1. Comparison of features and design aspects of µFP classified into bulk and surface micromachined devices.

	Bulk Micromachined filters	**Surface Micromachined filters**
Basic technology	two or more wafers, wafer bonding with spacer layer	one wafer, sacrificial layer etching
Design flexibility for the reflectors	high	low
Identical (matched) reflectors	yes	no (yes*)
Anti reflection coating (ARC) required	yes, both sides	on lower substrate (no ARC needed*)
Stiffness / flatness of the reflectors	high, no static and dynamic deformations	low, static and dynamic deformations
Moving mass, acceleration sensitivity	higher, not neglectable	very low, neglectable
Design flexibilty for electrostatic actuation and tuning range	higher	lower
Chip size, aperture size	larger	smaller
Complexity and costs of fabrication	higher	lower

* if the substrate of the lower reflector is removed.

3. COMPARISON OF TECHNOLOGY APPROACHES

There are two main technology approaches that can help to classify different implementations for µFPF, bulk micromachined and surface micromachined devices. Both of them have several pros and cons, which should be discussed here. However, some of developments described in next section have features of both approaches. Figure 2 shows typical cross sections of both versions and table 1 compares the most important design aspects and features.

Bulk micromachined µFPF are usually constructed of two or more wafers, which are structured by means of wet and dry etching, deposition of electrodes and optical layers and finally are bonded together to form the FP cavity. The cavity spacing is realized by additional spacer layers or by etching of gaps. Both reflectors are supported by the thick and mechanically stiff substrates, which helps to avoid warping due to layer stress and ensures flatness during actuation. The back sides of the substrates have to be anti-reflection coated (ARC).

With this structure it is possible to separate the actuation electrodes from the reflectors (different spacings) and thus mechanical tuning can be designed more flexible according to the desired spectral tuning range. The mass of the movable reflector plate usually cannot be neglected and makes the filter sensitive to external acceleration forces, which should be addressed by the design or requires additional compensation. While design and fabrication are more complex, such filters have the potential for better performance figures regarding tuning range, resolution and larger aperture sizes.

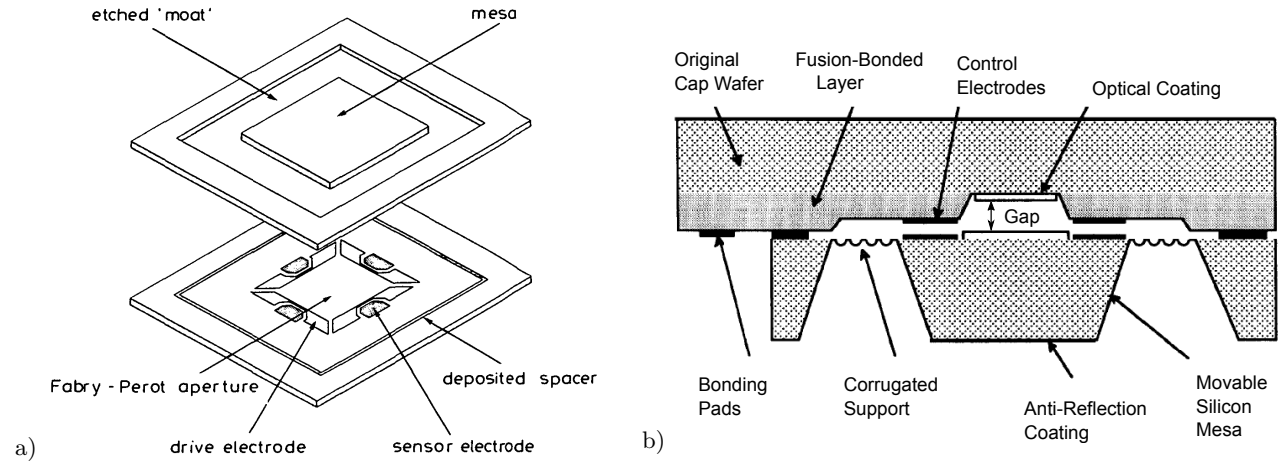

Figure 3. Bulk micromachined µFPF for WDM published by British Telecom and IC Sensors Inc.; a) Exploded view of the first generation devices (Reproduced by permission from Ref.[8], ©1987 The Institution of Engineering & Technology); b) Schematic cross sectional view of the improved second generation with corrugated diaphragm support (Reproduced by permission from Ref.[14], ©1991 Elsevier).

Surface micromachined µFPF are usually monolithically fabricated from only one wafer. A stack of layers to form electrodes, a spacer and the reflectors is deposited on one side. The spacer acts as a sacrificial layer, which is afterwards partly etched to release one of the reflectors as a free standing membrane. Optionally the substrate beneath the other (fixed) reflector can also be removed. Otherwise, the backside of the substrate has to be anti-reflection coated. Furthermore it is difficult to create perfectly matched reflectors with the substrate remaining in place, which decreases the optical efficiency of the FPI structure.

The spacing between electrodes and reflectors is identical, which limits the tuning range due to the pull-in phenomenon. In some of the developments reviewed here, the reflectors itself act as the control electrodes. Free standing membrane reflectors have to be tensioned and symmetrically layered to avoid warping. This imposes quite strict constraints on the choice of materials and the optical design. Nevertheless, membrane reflectors tend to bow under actuation forces. As a result the finesse decreases during tuning and the usable aperture is limited. On the other hand, the mass of the membrane can be neglected and therefore no acceleration effects can arise. This in turn gives room for a design with smaller electrodes and lower actuation voltages and last but not least, a smaller overall chip size. Compared to the bulk micromachining approach, the technology is much simpler and cost effective, which makes it best suited for mass production.

3.1 Bulk micromachined FP filters

3.1.1 British Telecom (UK) & IC Sensors Inc. (US)

To the best of the authors knowledge, the first publication on µFP devices dates back to 1987. Mallinson and Jerman[8] created a µFP for wavelength division multiplexing (WDM) in the spectral range of $1.3 - 1.5\,\mu m$. The movable reflector was supported by a mesa structure, suspended by a flexible membrane, which was etched out of the silicon substrate (figure 3a). Four separated actuation electrodes and additional sensing electrodes were used for closed loop control with capacitive feedback. The µFP was operated in the first interference order and achieved an effective finesse of about $\tilde{F}_E = 93$ ($FWHM = 3.1\,nm$). The membrane suspension results in a large chip size of $13 \times 15\,mm^2$.

The second generation was improved by replacing the membrane by a corrugated diaphragm (figure 3b) and as a result the chip size has shrunk to $5 \times 5\,mm^2$.[14] The aperture size was $1.4 \times 1.4\,mm^2$. With the new design interference orders $m = 8 \ldots 10$ and a reflector spacing of about $25\,\mu m$ were used. To maintain the high optical quality of the unprocessed polished wafers, the optical gap was not etched, but an additional wafer was fusion bonded and thinned as a spacer. The filter bandwidth was improved to $FWHM \approx 1\,nm$ while the finesse dropped to $\tilde{F}_E = 40$.

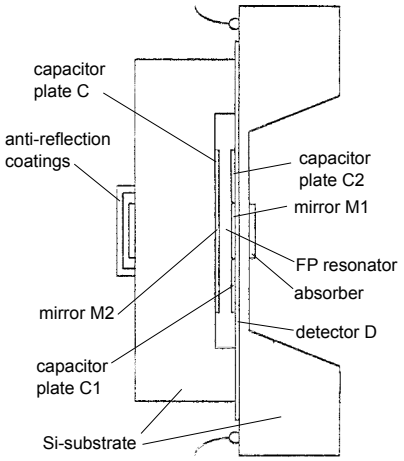

Figure 4. Schematic cross section of a µFP-sensor on chip reported by Rossberg (Reproduced by permission from Ref.[9], © 1995 Elsevier).

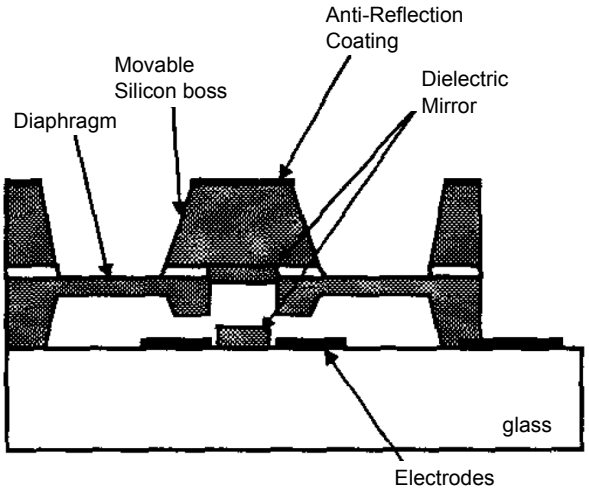

Figure 5. µFPF for WDM from Yokogawa (Reproduced by permission from Ref.[17], © 2002 IEEE).

3.1.2 Technical University of Munich (DE)

One of the first developments intended for the use in infrared spectroscopy was reported by Rossberg in 1995.[9] The basic construction (figure 4a) is very similar to the first generation devices from Mallinson and Jerman (see above). But instead of dielectric reflectors he used sputtered aluminum to create very broadband reflectors for the wavelength range $1.5 \ldots 7.5\,\mu\text{m}$. Unfortunately, the measured reflectance was relatively low $R \approx 0.85$ (reflective finesse $\tilde{F}_\text{R} \approx 20$) and the absorption was high ($A \approx 10\%$)[15]. A spectral resolution of 200 nm was calculated, with a drop of the peak transmittance down to $T_\text{peak} < 10\%$ with increasing wavelength. The most interesting fact of this work is, that for the first time on-chip integration of a thermopile infrared detector together with the µFPF was reported.[16]

3.1.3 Yokogawa Electric Corporation (JP)

Again quite similar to the work of Mallinson and Jerman (see above) the Japanese Yokogawa Electric corp. presented a µFPF for WDM around 1.5 µm.[17] Here the movable portion was made out of an SOI wafer, where the cavity spacing was defined by the thickness of the device layer and the buried oxide (figure 5) and the restoring force was provided by partially etching the wafer to a 10 µm thin membrane. The fixed reflector was supported by a glass substrate with four separated control electrodes. Electrode and reflector spacings were split up by different etching depths, by which the actuator design was optimized to the desired tuning range. The filter bandwidth was reported to be $FWHM = 0.5\,\text{nm}$, the free spectral range was $FSR = 35\,\text{nm}$. From this, an interference order of $m \approx 35...40$ can be deduced. The chip size was $6.2 \times 7.2\,\text{mm}^2$, the filter aperture can be estimated to be around 0.5 mm.

3.1.4 Axsun Technologies Inc. (US)

Axsun Technology Inc. developed an NIR spectrometer based on a narrow band tunable infrared light source, which is realized by the combination of a superluminescent diode (SLED) and a µFPF.[18,19] The movable portions of the filters are based on flexible silicon membranes and spiral tethers (figure 6b) which are structured out of SOI wafers. Various designs are described in the patent literature[20,21] including one with two identical membranes that are bonded together with an additional intermediate spacer. This particular design has the advantage, that the reflectors will move in the same direction under the influence of external acceleration forces. The aperture size is 200 µm. Another patent describes a dualband reflector made of two stacked DBRs with additional matching layers.[22] The µFPF can be operated simultaneously in both bands, one for the actual measurement and the second for wavelength referencing. The complete system consisting of the light source, µFPF, lenses, beamsplitters and a detector is set up on a thermally stabilized micro-optical bench (figure 6a).

a) 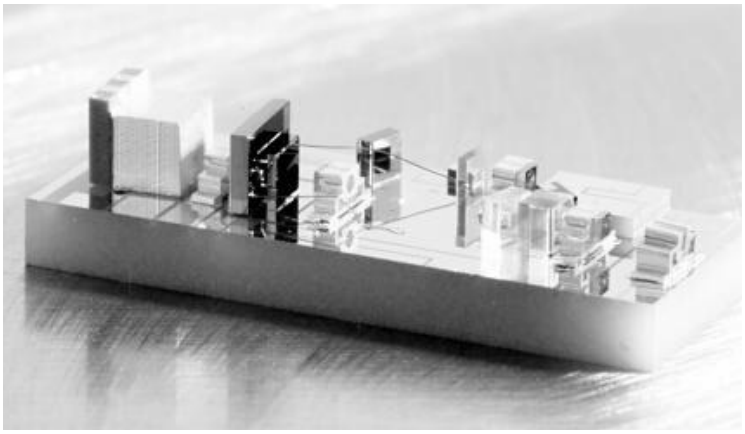 b) 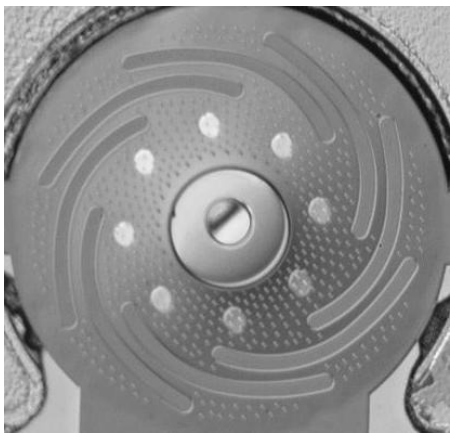

Figure 6. NIR microspectrometer with tunable SLED from Axsun: a) complete system on a micro-optical bench; b) flexible membrane and reflector of the µFPF (taken from Ref.[23]).

Various devices for different spectral ranges within $1350 \ldots 1800\,\mathrm{nm}$ and a spectral resolution of $3.5\,\mathrm{cm}^{-1}$ (0.1 nm) are available. In Ref.[4,19,23] a spectral resolution of 0.025 nm and a free spectral range of $FSR = 100\,\mathrm{nm}$ were reported. This would correspond to a remarkably high finesse of about $\tilde{F} = 4000$.

3.1.5 InfraTec GmbH, TU Chemnitz, Fraunhofer ENAS (DE)

The authors of this paper started to work in field of µFPF in 2001. In the very first concept the filter should have been constructed by four stacked wafers, where the lower wafer supports the fixed reflector and the inner two form the movable part. The latter was suspended by parallel beams arranged in pairs, which was supposed to ensure a perfect linear movement without any tilt. Four pairs of control electrodes on the outermost wafers were intended to linearize the actuation characteristics and to move the inner portion in both directions[24] (figure 7).

The complexity of the design and fabrication led to several simplifications in the following work, finally resulting in a two wafer design similar to that described in the previous sections.[25,26] To that time the wafers were bonded by an intermediate SU-8 layer, whereas filter designs developed more recently use silicon fusion bonding.[27]

The overall chip dimensions were $8.5 \times 8.5\,\mathrm{mm}^2$ with an large filter aperture of about $2 \times 2\,\mathrm{mm}^2$. DBRs of silicon and SiO_2 layers with two and three periods ($[HL]^2$ and $[HL]^3$) were tested.[25] The layers were deposited by CVD (chemical vapor deposition) and structured by standard photolithography and etching. The two period design provided better overall optical performance, which was due to lower layer stress and roughness on the one hand and better matched reflectivity on the other. Two types of first order µFPF spanning tuning ranges of approximately $3 - 4\,\mu\mathrm{m}$ and $4 - 5\,\mu\mathrm{m}$ were successfully fabricated and characterized (figure 8a). The measured filter bandwidths were $FWHM = 60 \ldots 100\,\mathrm{nm}$ and $80 \ldots 120\,\mathrm{nm}$, from which an effective finesse of $\tilde{F}_\mathrm{E} = 40 \ldots 60$ was deduced.[26]

The µFPF is integrated into a TO-8 package together with a pyroelectric infrared detector resulting in a tiny hermetically sealed microspectrometer module (figure 8b). The $2 \times 2\,\mathrm{mm}^2$ size of the sensing pyroelectric element is matched to the filter aperture. An additional wide bandpass filter, which is always needed to block unwanted radiation (e.g. from higher orders), is integrated into the cap.

Electrode size and spring stiffness were designed for a maximum control voltage of about 35 V. The mass of the movable part is about 12 mg, which results in an acceleration response of the filter wavelength of up to 40 nm/g (with $\mathrm{g} = 9.81\,\mathrm{m/s}^2$). To compensate for this closed loop control with capacitive feedback has been applied by means of an integrated ASIC and external driving electronics.[29] An appropriate calibration scheme allows to compensate for temperature drifts as well. The filter wavelength can therefore be stabilized to less than 5 nm under varying environmental conditions. Spectral calibration data are stored in an EEPROM, which is also integrated in the package. Such microspectrometer modules are commercially available from InfraTec together with driving electronics and software.[30]

In further development work the reflector materials silicon and SiO_2 were replaced by germanium, zinc sulfide and a metal fluoride. The layers are deposited by ion assisted evaporation (IAD), which is a standard technology in the fabrication of thin film interference filters. The new three material system enables much more design options to precisely adjust the reflectance (reflective finesse) and for stress compensation. In this way the spectral coverage of the µFPF was expanded to the LWIR spectral range. Standard single-band filter designs for first order operation as well as dual-band filters for simultaneous tuning in the mid and long wave infrared were designed and fabricated.[28,31] Optical measures in terms of finesse and throughput are comparable to the previously developed filters. A dual-channel pyroelectric detector was developed and the 3D integration of a beamsplitter and blocking filters were realized for packaged dual-band devices (figure 9).

In recent years devices with improved resolution and dynamics were developed, especially intended for the fast analysis of hydrocarbon gas mixtures. An *FWHM* filter bandwidth down to 20 nm and a tuning range of $3.1 - 3.7\,\mu m$ were achieved with 4^{th} order filters. To compensate for the loss in throughput and to enable fast scanning, the filters were combined with lead selenide photoresistors.[32] A new fast scanning method and a gas sensor demonstrator implementing the same were presented.[33]

Although closed loop control works very well to encounter the acceleration sensitivity a complete new MEMS design with two movable reflectors has been developed too. The major advantage of such a structure is, that the reflectors move in the same direction under the influence of external acceleration forces from gravity or vibrations (compare to Axsun). As a first consequence the suspension can be made softer. Secondly, both reflectors have

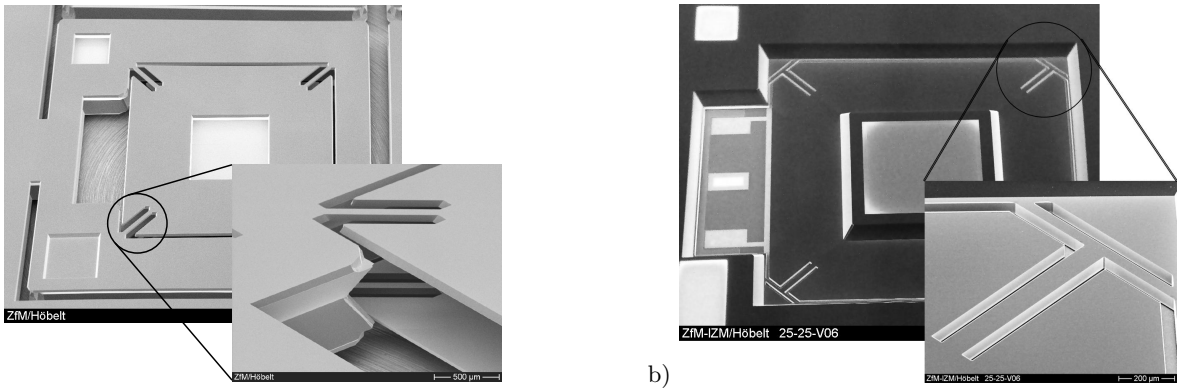

a) b)

Figure 7. SEM images of µFPF from InfraTec GmbH, TU Chemnitz and Fraunhofer ENAS with detailed view of the suspension structures: a) first generation design with parallel beam arrangement; b) second generation design with T-shaped suspension beams (taken from Ref.[26]).

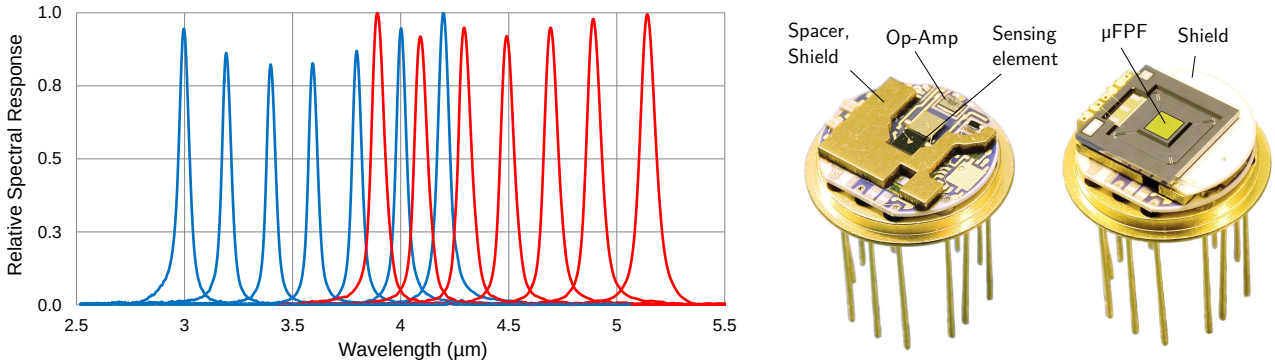

a) b)

Figure 8. Integrated microspectrometer modules from InfraTec: a) Spectral response of two types with tuning ranges in the MWIR region (indicated by the colors blue and red); b) Inside view of the modules with pyroelectric detector (left) and the µFPF mounted above (right) (taken from Ref.[28]).

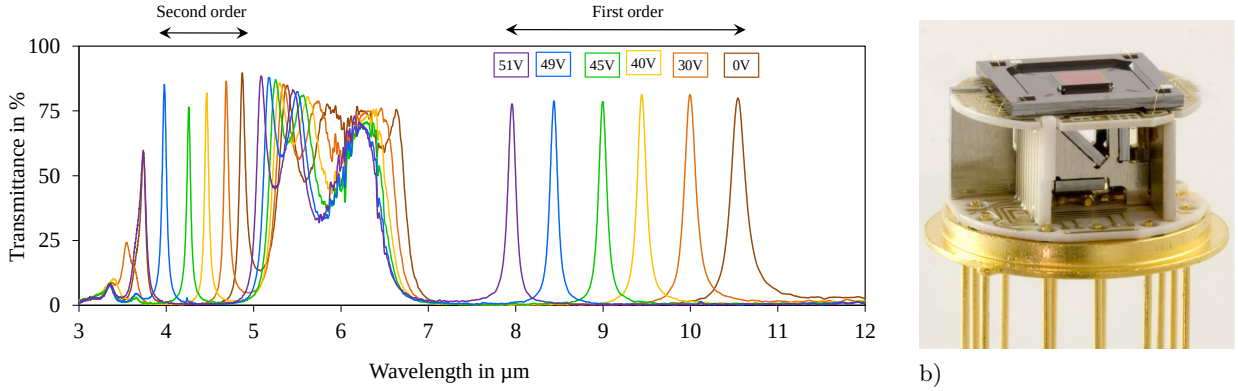

Figure 9. Dual-band µFPF for the mid and long wave infrared: a) transmittance spectra of the filter; b) prototype of the dual-channel microspectrometer module (taken from Ref.[28])

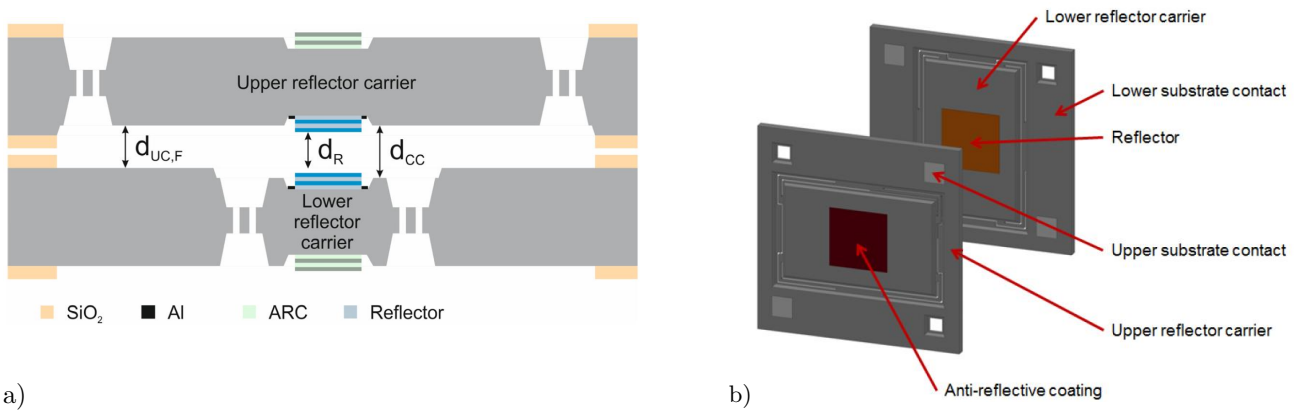

Figure 10. Bulk micromachined µFPF with two suspended reflector carriers (second generation): a) schematic cross section; b) exploded view of the two wafers (taken from Ref.[35]).

to move only half the way compared to conventional designs with only one suspended reflector. As a result of both effects, the electrodes can be made smaller and the chip dimensions can be shrinked without sacrificing the optical aperture size. The reflector carriers are rectangular shaped and arranged perpendicular to each other. This way they partly overlap with the fixed frame and form an air gap, that can absorb mechanical shocks (figure 10). Up to now, two design generations have been reported.[34,35] In the current development state a simplified structure and fabrication process as well as a chip size of $7 \times 7\,\mathrm{mm}^2$ were achieved. Two optical filter designs, a mid and long wave dual-band version and higher order design with increased resolution (both designs similar to that described above) have been realized.

One of the major cost-drivers of the technology described above is the fabrication of the optical coatings. Therefore further research was directed to replace the dielectric thin film layers by subwavelength gratings. A reflector can be created by an array of specially designed dielectric or metallic patches supported by a thin membrane. The optical properties (wavelength range, stop-band width and reflectance) predominantly depend on the pitch and the shape of the arrayed pattern and secondly on the material properties. Such structures can be fabricated by nano imprint lithography (NIL), which potentially result in significant cost savings.

In this work, arrays of 100 nm thick aluminum ring or disc resonators on a 200 nm thick silicon nitride membrane for the wavelength range $2.5 - 5\,\mu\mathrm{m}$ were investigated (figure 11). Finite Difference Method (FDM) analysis was used for simulations, e-beam lithography and NIL for the fabrication.[36–38] It was found that, due to the absorption in the metal resonators, the reflectance should not be too high, otherwise, the transmittance of the filters would drop dramatically.

Based on the existing MEMS design with one movable reflector tunable filter prototypes operating in the 3$^{\mathrm{rd}}$ to 5$^{\mathrm{th}}$

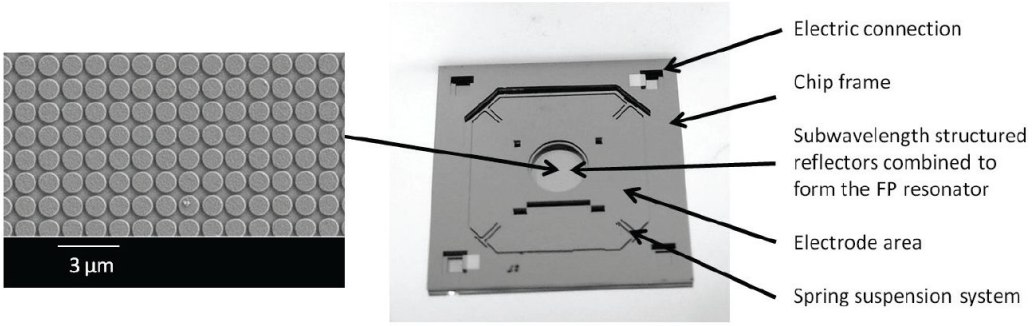

Figure 11. µFPF with subwavelength grating reflectors; left: SEM image of the disc resonators fabricated by NIL; right: photograph of a prototype (Reproduced by permission from Ref.[38], ©2015 Elsevier).

interference order were realized. The membranes were released by backside etching of the silicon substrates, which at the same defined the optical aperture. White-light interferometric measurements proved excellent planarity and roughness over the entire aperture. Measurement and simulation results of $FWHM$ and transmittance agreed quite well. Compared to filters with DBRs, the finesse is low ($\tilde{F} = 10 \ldots 15$) but in accordance to the low reflectivity design. It doesn't degrade when the filter is tuned, because the membrane is supported by a rigid silicon frame and completely separated from the actuation electrodes. Due to these results, the approach seems to be a good candidate for large aperture filters with low finesse but high throughput in hyperspectral imaging.

3.1.6 Teledyne Scientific & Imaging LLC (US)

Around 2003 a development was started at Rockwell Scientific (now operated under the name Teledyne Scientific & Imaging LLC) directed towards arrayed µFP filters combined with an IR focal plane array (FPA) for spectral imaging applications.[40] The core of the concept included the following aspects: Filter elements with an optical aperture of $200 \times 200\,\mu m^2$ up to $400 \times 400\,\mu m^2$, each of them covering groups of detector pixels, can be individually addressed and tuned over the range $8 - 10\,\mu m$. At the same time they provide a high transmittance (without tunability) in a second spectral band of $3 - 5\,\mu m$. Because of this properties the system has been denoted as *dual band adaptive focal plane array*. Fabrication of the filter devices was as follows: A first reflector was coated on a silicon wafer and patterned by lift-off. The same was done for the second reflector on top of the device layer of an SOI wafer and suspension structures were patterned. The two wafers were bonded together by Au-Au thermocompression bonding, the handle wafer was removed and AR coatings were added afterwards (figure 12a). The reflectors and AR coatings made of germanium and zinc sulphide multilayers were optimized in such a way, that stress and bow are minimized at the detectors operation temperature of 77 K (liquid nitrogen cooling). Various test designs were fabricated and tested. Transmittance measurements were carried out with several

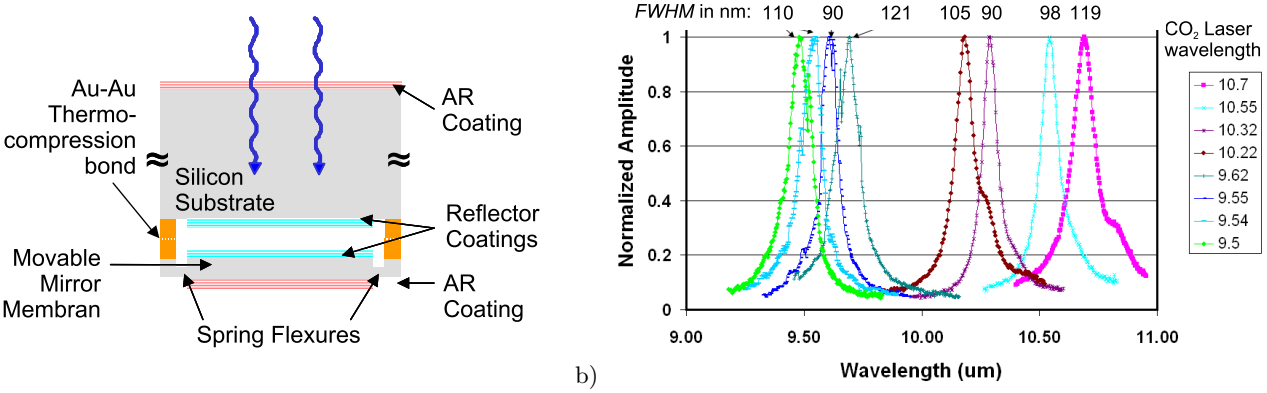

a) b)

Figure 12. µFPF for dual band adaptive focal plane array from Teledyne Scientific: a) Schematic cross section of a single filter element; b) transmittance spectra measured with CO_2 lasers (taken from Ref.[39]).

CO_2 lasers (collimated beam) and voltage control of the filters. Because the voltage was directly applied to the reflectors the tuning range was limited to $9.5 - 10.7\,\mu m$ due to the pull-in effect. $FWHM$ values of $90 \ldots 120\,nm$ were reported from this measurements (figure 12b), which corresponds to a high finesse of $\tilde{F}_E = 60 \ldots 80$.[41–43] By means of a charge control actuation method instead of voltage control to tuning range was extended up to $8 - 11\,\mu m$.[39]

3.2 Surface micromachined FP filters

3.2.1 VTT Technical Research Centre of Finland (FI)

In 1997 the CO_2-CarboCap sensor of the Finnish company Vaisala OY was launched. It was the first commercialized gas sensor product based on a µFPF.[44] The µFPF was developed in cooperation with VTT. The upper flexible membrane reflector consisted of three $\lambda/4$ layers of poly-silicon and SiO_2 (HLH), the lower fixed reflector was supported by a silicon substrate and was made of two layer periods ($[HL]^2$). The sacrificial spacer layer was made of SiO_2 too. The outermost layers were doped to provide electrically conductance as control electrodes (figure 13a). Circularly shaped electrodes located on the substrate were used to minimize the warpage of the membrane during actuation[45] (figure 13b).

The filter was tuned in the first interference order ($m = 1$) over a the spectral range $3.9 - 4.6\,\mu m$ (CO_2 absorption around $4.26\,\mu m$) and achieved a bandwidth of about $FWHM \approx 70\,nm$, which corresponds to a effective finesse of about $\tilde{F}_E \approx 40$. The aperture diameter was 1 mm, the chip size was $3.3 \times 3.3\,mm^2$.[10,46,47] In the gas sensor it was combined with a thermopile detector.

In Ref.[48] a special method for the measurement of the gas absorption has been described: Here the filter is not scanned continuously to acquire spectra but the filter wavelength is switched cyclically between the absorption band of CO_2, a reference wavelength without any absorption and the blocking range of an additional long pass filter in front of the µFPF. With this method the filter not only acts as wavelength selective element but also as a modulator. At the same time the long pass filter is utilized as a wavelength reference to compensate for temperature drifts of the µFPF. Other publications describe a method with a pulsed thermal emitter.[49]

The technology described so far has been adapted for other applications in the range $2.8 \ldots 5\,\mu m$, e.g. for the measurement of hydrocarbon gases and water vapor. In Ref.[50] a TE-cooled PbSe photoresistor was used. The µFPF was mounted directly on top of the detector for temperature stabilization (figure 14a). In later publications[51] the µFPF was placed on a PCB in front and outside of the housing of an uncooled PbSe detector. For this filter version an $FWHM$ bandwidth of $50 \ldots 60\,nm$ over a tuning range of 2.8-3.5 µm in the first inteference order were reported. The chip size was $4 \times 4\,mm^2$ with a large optical aperture of 2 mm. Based on s similar design, a CO_2 sensor for cell phones (as a clip-on device) has been demonstrated quite recently.[52]

Further development work at VTT has transferred the technology to other wavelength ranges and application fields.[5,53] Particular emphasis is placed on µFPF for the visible range, especially for hyperspectral imaging. Here the reflectors are made from very thin layers of TiO_2 and Al_2O_3 fabricated by atomic layer deposition (ALD). A photoresist is used as sacrificial spacer layer, a quartz wafer act as the substrate.[54] Aperture sizes of up to 2 mm have been reported.[55] The effective finesse of various µFPF with interference orders $m = 2 \ldots 6$ was around

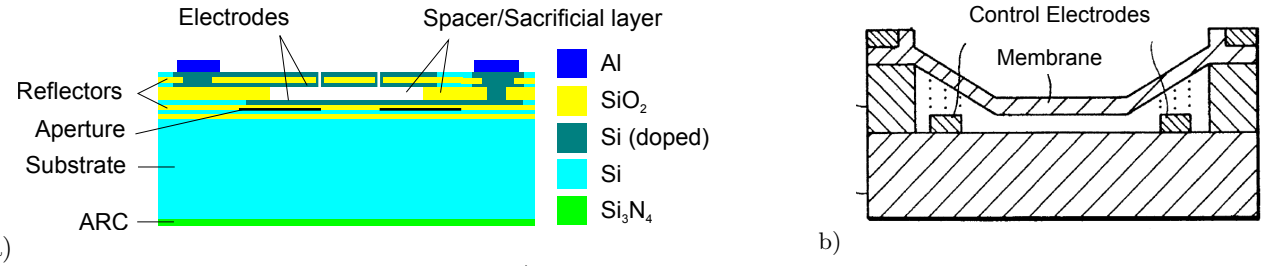

a) b)

Figure 13. µFPF from from VTT and Vaisala; a) Schematic cross section of the surface micromachined MEMS filter, (taken from Ref.[46]); b) Electrode configuration to prevent warping of the reflector membrane (taken from Ref.[45]).

a)

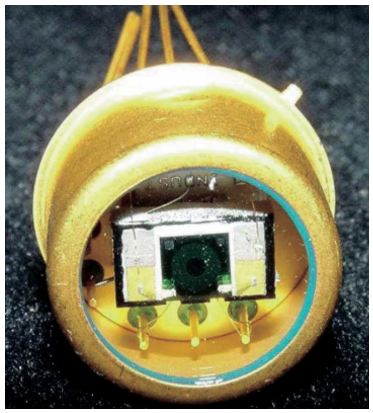

b)

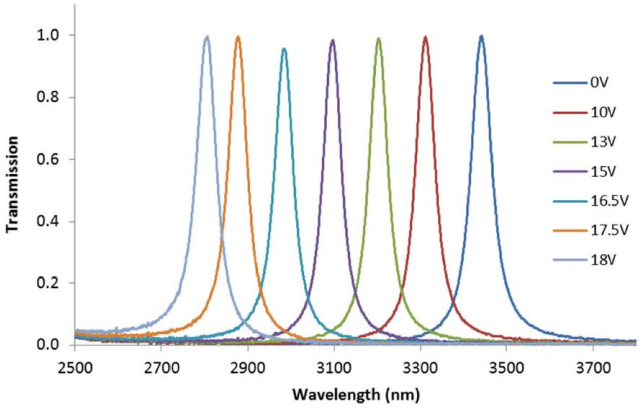

Figure 14. µFPF sensors from VTT for hydrocarbon gases and water vapor; a) µFPF integrated on top of a TE cooled IR detector in a TO-8 housing (taken from Ref.[50]); b) Normalized transmittance spectra of a µFPF with tuning range 2.8-3.5 µm (taken from Ref.[51]).

$\tilde{F}_\mathrm{E} \approx 30$, significantly lower than expected from simulations. The main reasons stated were bending of the highly tensile-stressed membrane under the influence of electrostatic forces and an inhomogeneous spacer layer.

To provide a sufficiently large tuning range, a capacitor is integrated on chip and connected in series to the actuator capacitance. This virtually enlarges the electrode spacing by utilizing an AC voltage driving scheme.

The low refractive index contrast of the materials TiO_2 and Al_2O_3 ($n_\mathrm{H}/n_\mathrm{L} \approx 1,4$) results in narrow stop band reflectors which are not able to cover the whole visible range ($\lambda \approx 380 \ldots 780\,\mathrm{nm}$). As a solution a cascaded configuration of two or more µFPF designed for different ranges and interference orders has been proposed.[55]

Another approach to overcome the ambiguities of the several peaks in higher order configurations has been described in Ref.[56] An image sensor with an RGB filter mosaic (BAYER pattern) is used. The orders of the µFPF are selected in such a way, that they match the spectral sensitivity of the three color channels (figure 15). It was firstly used in hyperspectral cameras with piezo actuated FP filters from VTT (not further discussed here, see also Ref.[57,58]), which had broadband silver mirrors.[59] It has been also applied to µFPF with TiO_2/Al_2O_3 DBRs[60] (figure 16), once again the useable range is limited by the stop band width of the reflectors.

Fabrication of very large membranes with diameters up to 10 mm for spectral imaging devices was also investigated. The membranes were made of low-stress polysilicon and silicon-rich silicon nitride (SiN) thin films.[61] Filters with TiO_2/Al_2O_3 ALD layers achieved aperture sizes up to 4 mm. A low effective finesse in the order of $\tilde{F}_\mathrm{E} = 7 \ldots 10$ was reported, although only a portion of the aperture was illuminated while testing the filter.

The monolithically integration of a PIN photodiode with a µFPF was reported in Ref.[62]

µFPF for near infrared ranges have been also developed at VTT. Polysilicon and silicon nitride are used for the reflectors. Several designs with aperture ranging from 0.5 to 1.5 mm have been reported.[53,63] From the measured *FWHM* values the finesse can be deduced to be in the order of $\tilde{F}_\mathrm{E} = 20 \ldots 30$.

In current research work at VTT Bragg reflectors are developed, which consist of $\lambda/4$ polysilicon layers (as the high index material) and $\lambda/4$ air gaps in between (low index layers). The air gaps are created by etching of a sacrificial SiO_2 layers. Anchors between the polysilicon layers provide a mechanically stable structure and preserve the heights of the air gaps after the release step (figure 17a). Due to the high refractive index contrast of silicon and air ($n_\mathrm{H}/n_\mathrm{L} \approx 3,4$) such reflectors exhibit very broad stop bands. With only three layers (*HLH*) a reflectance of about $R \approx 96\%$ can be achieved. Furthermore the reflectors have low losses up to the long wave infrared (in contrast to the formerly used low index materials silicon oxide or silicon nitride) and can therefore be used for µFPF up to 11 µm.[64] The complete FP filter structure consists of at least four polysilicon layers and three sacrificial SiO_2 layers, which have to be etched in one or several release steps (figure 17b).

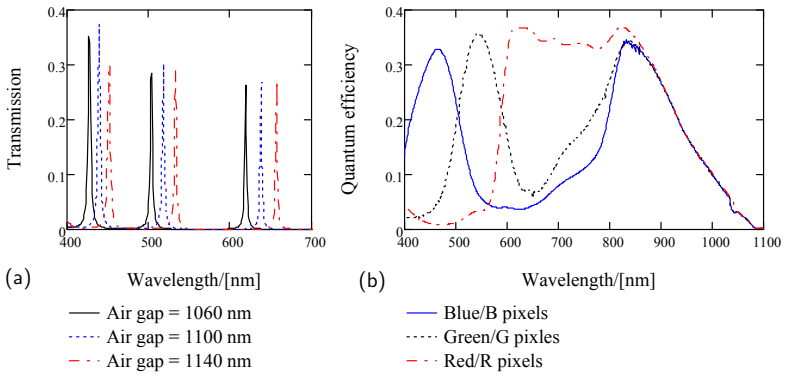

Figure 15. Simultaneous use of three interference orders of an FP filter matched to the channels of an RGB image sensor: a) filter transmittance; b) spectral sensitivity of the red, green and blue sensor channels (taken from Ref.[59]).

Figure 16. µFPF for the visible range mounted on a TO-8 header to be used in a handheld hyperspectral imager (taken from Ref.[60]).

Publications about first order long wave µFPF state a tuning range of $7.5-9.5\,\mu m$ and a bandwidth of $FWHM = 115\ldots135\,nm$. This corresponds to a high finesse of $\tilde{F}_E \approx 50\ldots60$. The aperture sizes range from 0.8 mm to 1.2 mm, the outer chip dimension are $4\times4\,mm^2$.[65,66]

µFPF with Si/Air reflectors for the mid wave infrared with tuning ranges of $3.7-4.5$ µm (CO_2 version) $2.7-3.5$ µm (CH version) have also been reported. In this work many efforts were taken to optimize the technology of sacrificial layer etching. Several combinations of etch rates and temperature, different oxide types as well as a sandwich structures have been tested. In terms of finesse the optical performance of the CH version was comparable to the long wave µFPF but significantly worse for the CO_2 version. Aperture and chip dimensions were identical to the long wave µFPF described above, but in contrast to the latter the substrate beneath the lower reflector has not been removed (reflectance mismatch) nor has it been anti-reflection coated. These facts may have affected the optical performance.

In 2013 the company Spectral Engines was spun off from VTT aiming for the commercialization of their µFPF technology for industrial applications. Several types of OEM sensor modules for near and mid wave infrared ranges are available.[67] In 2015 the Japanese Hamamatsu Photonics has launched an NIR spectral sensor based on the VTT µFPF technology and an InGaAs detector packaged together in a TO-5 housing.[68] The tuning range is $1.55-1.85\,\mu m$ with a spectral resolution of about 20 nm. The filter aperture diameter is 0.75 mm, but the active area of the detector is even smaller (0.1 mm).

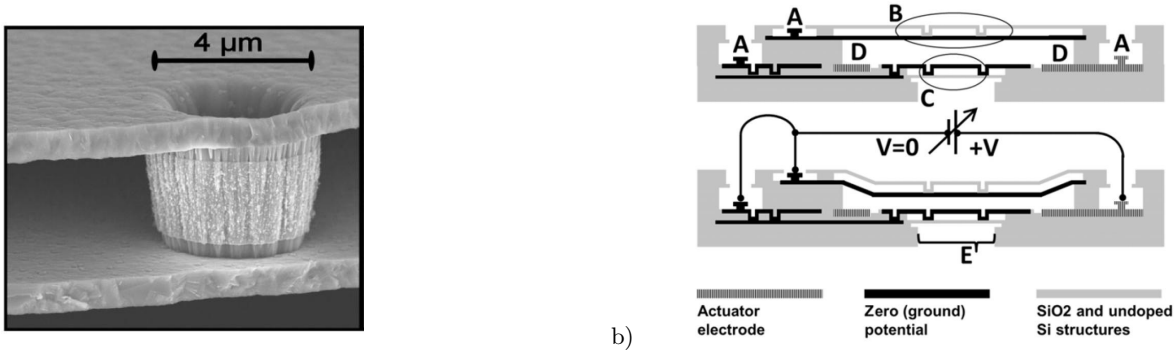

Figure 17. µFPF from VTT with Si/Air Bragg reflectors: a) SEM image of the Si/Air/Si with one of the anchors (Reproduced with permission from Ref.[64] Copyright 2011, IOP Publishing); b) schematic cross section of a long wave infrared µFPF in rest position and actuated by a control voltage (Reproduced by permission from Ref.[65], ©2012 IOP Publishing).

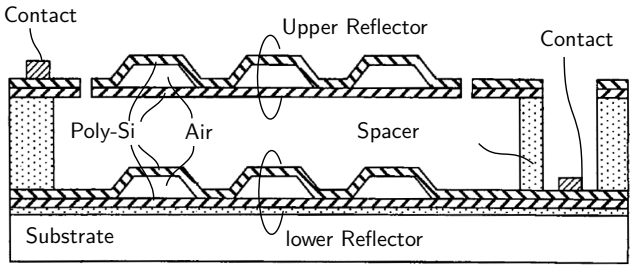

Figure 18. Schematic cross section of a µFPF from Denso Corp. with Si/Air Bragg reflectors (taken from Ref.[70]).

3.2.2 Denso Corporation (JP)

The Japanese Denso Corp. has developed a surface micromachined µFPF with Si/Air Bragg reflectors. The basic technology and the design are very similar to that from VTT (see above), but in contrast, the *HLH* layer stack is comprised of a hexagonal honey-comb structure instead of planar layers and anchors (figure 18). The diameter of the optical aperture is 0.8 mm, the overall chip size is about $4 \times 4\,\mathrm{mm}^2$. The spectral width of the reflectors is very broad ($3.2 \ldots 8.4\,\mu\mathrm{m}$). Practical results of a first order µFPF with a tuning range of $3.2 - 4.5\,\mu\mathrm{m}$ has been reported. The filter bandwidth was $FWHM \approx 60\,\mathrm{nm}$ ($\tilde{F}_\mathrm{E} \approx 60$), but the measured peak transmittance was relatively low ($T_{pk} = 10 \ldots 40\%$).[69,70] It can be assumed, that the reasons lies in the honeycomb structure, which limits the effective aperture area.

The target application is gas sensing in vehicles, with a broad variety of gases (CO_2, CO, NO_x, SO_2, C_2H_5OH).[69,70] Ref.[71] describes a special configuration of the control electrodes to enable the very large tuning ranges, that are required for this application.

3.2.3 Yokogawa Electric Corporation (JP)

Beside the bulk micromachined µFPF for WDM, the same group at Yokogawa (see above) has also developed a surface micromachined filter for sensing CO_2 and water vapor in the spectral range $2.5 - 4.5\,\mu\mathrm{m}$.[72] The upper membrane reflector of the MEMS device is a three layer sandwich of polysilicon, silicon nitride and polysilicon with an overall thickness of $\lambda/4$ at the reference wavelength 3.5 µm. The fixed reflector is a single *LH* layer period of SiO_2 and polysilicon on a silicon substrate. SiO_2 is also used as the sacrificial layer. The diameters of the whole reflector membrane, which also serves as the control electrode, and the optical aperture are 1.8 mm and 0.8 mm respectively (figure 19a).

The sensor uses three spectral channels: at 4.3 µm CO_2 is measured using the first interference order of the µFPF, 2.7 µm is used for the water measurement and 3.3 µm as the reference channel, both in the second interference order. The finesse is already low ($\tilde{F} \leq 10$) at the flat rest position of the reflector membrane and is further decreases when the filter is tuned (figure 19b).

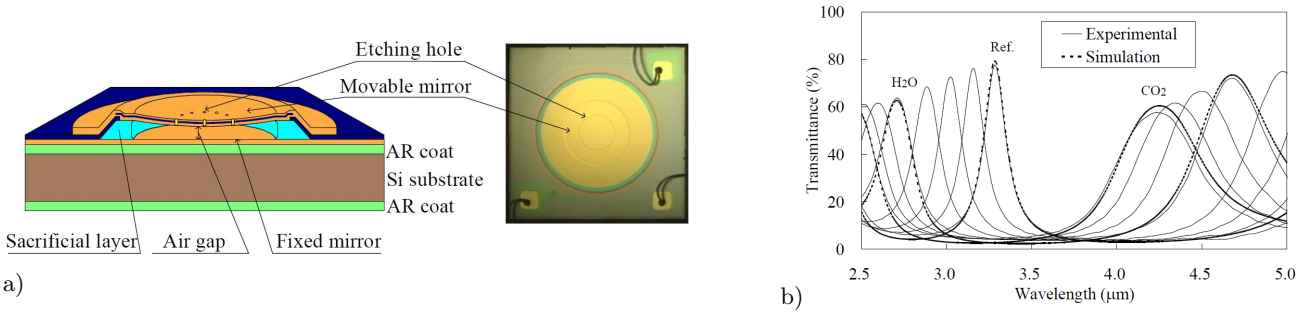

Figure 19. Surface micromachined µFPF from Yokogawa for CO_2 and H_2O sensing: a) Schematic cross section and photograph of the chip; b) Comparison of simulated and measured transmittance spectra (Reproduced with permission from Ref.[72], ©2003 IEEE).

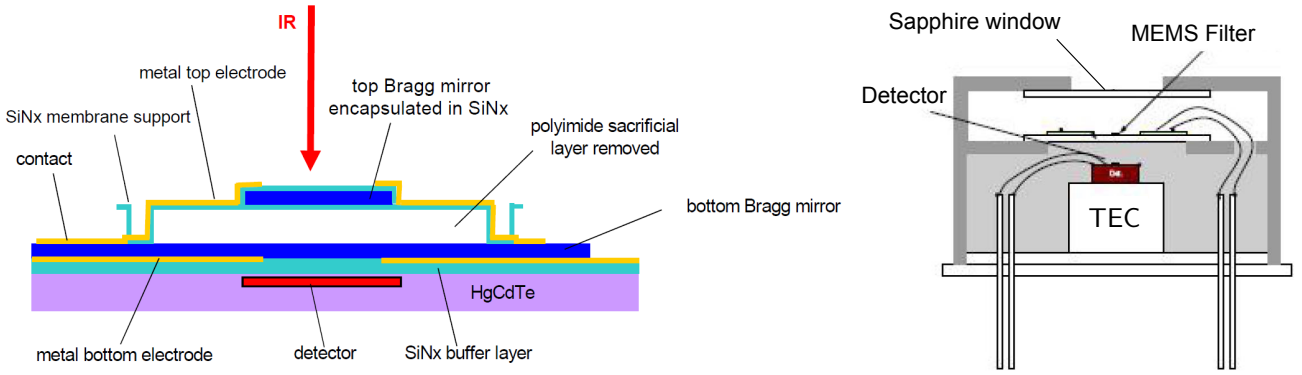

a) b)

Figure 20. µFPF of the Western University of Australia: a) schematic cross section with integrated MCT detector; b) integrated sensor module in a TO-8 housing (taken from Ref.[74]).

3.2.4 University of Western Australia (AU)

A research group at the University of Western Australia is working in the field of µFPF for many years. First devices were developed for near and mid wave infrared ranges[73–76] and very recently also for the long wave infrared.[77] The initial idea was to monolithically integrate a µFPF and an mercury cadium telluride (MCT) focal plane array.[73,78]

The first design was based on Ge-SiO Bragg reflectors (*HLH*), which were deposited by thermal evaporation and encapsulated by a SiNx layer. For a single pixel an aperture of $100 \times 100\,\mu m^2$ was sufficient. For first sensor prototypes a hybrid integration with the detector chip in a TO-8 package was realized (figure 20). Two filter versions with narrow tuning ranges of $1.8 - 2.2\,\mu m$ and $3.6 - 4.5\,\mu m$ (limited by pull-in) were fabricated. The *FWHM* bandwidths were about 100 nm and 200 nm, which corresponds to a low effective finesse of $\tilde{F}_E \approx 17$ and was mainly caused by the curvature of the mirrors.

A new actuator design with a so-called double supported beam structure was developed, which led to an increased tuning range $1.6 - 2.4\,\mu m$ and improved spectral resolution.[79,80] In Ref.[81] the number of layers were increased (*HLHLH*) resulting in a relatively high reflectance finesse of about $\tilde{F}_R \approx 130$. Because the curvature of the released reflector (defect finesse) was not improved at the same time, the effective finesse ($\tilde{F}_E < 20$) and peak transmittance ($T_{pk} < 20\%$) were low.

In recent work Si/Air Bragg reflectors ranging in size from $200 \times 200\,\mu m^2$ up to $5 \times 5\,mm^2$ were designed and fabricated. They showed good optical performance and a filter structure similar to that shown in figure 20a has been proposed. Measurements of the reflector surface profile indicate, that the inner portion of about 1.5 mm of a $2 \times 2\,mm^2$ reflector is flat enough to be used for a µFPF.[76,82]

Very recently a new approach for µFPF with a reflector membrane consisting of only a single quarterwave germanium layer has been presented.[77] The fixed lower reflector is a double period $[HL]^2$ of Ge and ZnS. The optical layers are thermally evaporated and a spun off polyimid layer acts as the spacer and sacrificial layer. The filters were designed for tuning ranges within $8 - 12\,\mu m$. The low reflectance of the upper single Ge layer and the mismatch to the lower reflector result in a quite low reflective finesse and a broad *FWHM* bandwidth of about 500 nm but also in a high peak transmittance of $\geq 80\,\%$. It has been stated, that such low spectral resolution is sufficient for hyperspectral imaging applications. Devices with different membrane sizes ranging from $200 \times 200\,\mu m^2$ up to $1000 \times 1000\,\mu m^2$ has been fabricated and characterized. Measurement results were compared to simulations, which include the bow of the reflectors during actuation. In rest position the predicted 500 nm were achieved. This resolution was also maintained during actuation for the smallest filter version, while the larger versions significantly suffered from the strong warpage of the membranes.

a) 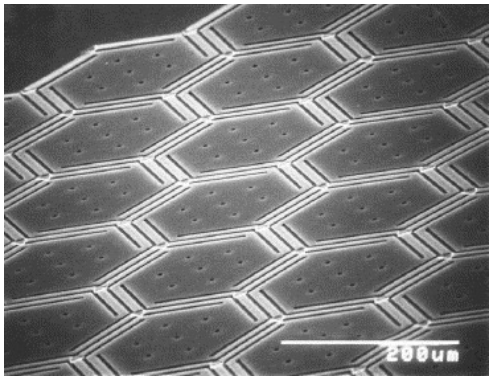

b) 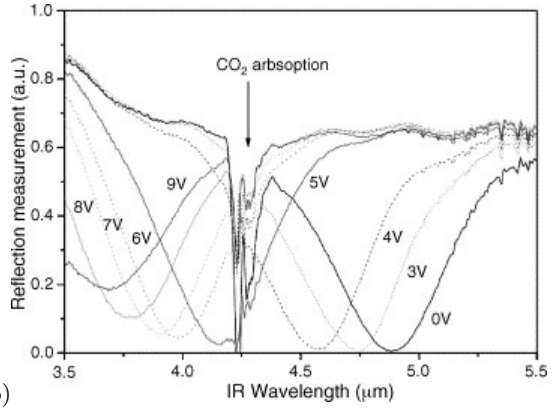

Figure 21. µFPF from IMB-CNM with a segment upper mirror: a) SEM photograph of the mirror; b) measured reflectance spectra of the filter device for different actuation voltages (Reproduced with permission from Ref.[83], ©2005 Elsevier).

3.2.5 Barcelona University, Institute of Microelectronics of Barcelona IMB-CNM (ES)

At the Centro Nacional de Microelectrónica (IMB-CNM) of Barcelona an alternative approach for a surface micromachined µFPF in a gas sensor has been developed. The upper reflector of the filter structure is segmented into individually suspended hexagonal shaped membranes with a size of about 200 µm (figure 21a). Both reflectors are made of single quarterwave layers of polysilicon. Between the lower reflector and the silicon substrate an anti-reflection layer was sandwiched to match the reflectance of both mirrors. For the measurement of CO, CO_2 and CH_4 a large tuning range of about $3.2 - 4.7\,\mu m$ is needed and consequently the first interference order was used. A thermopile detector also fabricated with MEMS technologies was flip-chip bonded to the filter. Although the technology was optimized for stress balancing and low warpage of the reflectors,[84,85] a low effective finesse of only $\tilde{F}_E \leq 10$ has been demonstrated (figure 21b).

4. DISCUSSION AND SUMMARY

A review of µFP filter technology for different applications in the infrared and beyond has been given. Two main fabrication approaches can be distinguished, surface and bulk micromachining techniques.

The first approach seems to dominate the published work especially over the recent ten years. It can be assumed, that this fact is mainly due to the relatively simple and low cost fabrication technology which makes it suitable for mass production. Another reason might be, that the suspended membrane mirrors are inherently insensitive to acceleration forces, which is a great advantage. However, there are also some drawbacks. The bow of the membrane mirrors results in some limitations on the aperture size (optical throughput) or the spectral resolution or even on both. This can be accepted to some extent for the visible and near infrared range, because small detectors with very high detectivity are available here. In the mid and long wave infrared the situation changes completely on the detector side and therefore large filter apertures are urgently required. This is in particular true for hyperspectral imaging with focal plane arrays.

Bulk micromachined filters on the other hand are considerably more complex and costly to fabricate, but they have the potential for better optical performance figures, larger aperture sizes and a more flexible design. Several approaches exist to encounter the acceleration sensitivity with good success. These facts make them a good choice for industrial applications, which are less cost-sensitive but require a high performance.

As far as can be judged today, both approaches will find applications but there is also still a lot of room for further improvements. However, commercial success depends on further very important aspects, which are usually not sufficiently addressed by scientific publications: calibration techniques and calibration transfer as well as compensation of temperature and long term drifts, to mention only a few.

5. ACKNOWLEDGMENT

Our own research was supported by the Federal Ministry of Education and Research (Germany). We thank all the authors and co-workers who have contributed to the research projects that has been discussed in this paper. Many thanks also to the authors and copyright holders, who gave their permission to reproduce figures.

REFERENCES

1. Crocombe, R. A., "Miniature optical spectrometers: There's plenty of room at the bottom, Part I: Background and mid-infrared spectrometers," *Spectroscopy* **23**(1), 38–56 (2008).
2. Crocombe, R. A., "Miniature optical spectrometers: Follow the money, Part II: The telecommunications boom," *Spectroscopy* **23**(2), 56–69 (2008).
3. Crocombe, R. A., "Miniature optical spectrometers, Part III: Conventional and laboratory near-infrared spectrometers," *Spectroscopy* **35**(5), 40–50 (2008).
4. Crocombe, R. A., "Miniature optical spectrometers: The art of the possible, Part IV: New near-infrared technologies and spectrometers," *Spectroscopy* **23**(6), 26–37 (2009).
5. Malinen, J., Rissanen, A., Saari, H., Karioja, P., Karppinen, M., Aalto, T., and Tukkiniemi, K., "Advances in miniature spectrometer and sensor development," in [*Proc. SPIE 9101 Next-Generation Spectroscopic Technologies VII*], 91010C (2014). http://dx.doi.org/10.1117/12.2053567.
6. Silva, D. K. K. M. B., Tripathi, D., Mao, H., Antoszewski, J., Nener, B. D., Dell, J. M., and Faraone, L., "Recent developments towards low-cost MEMS spectrometers," in [*Proc. SPIE 9101 Next-Generation Spectroscopic Technologies VII*], 910108 (2014). http://dx.doi.org/10.1117/12.2053505.
7. Fabry, C. and Perot, A., "Sur les franges des lames minces argentées et leur application à la mesure de petites épaisseurs d'air," *Ann. Chim. Phys* **12**, 459–501 (1897).
8. Mallinson, S. R. and Jerman, J. H., "Miniature micromachined Fabry-Perot interferometers in silicon," *Electronics Letters* **23**(20), 1041–1043 (1987). http://dx.doi.org/10.1049/el:19870728.
9. Rossberg, D., "Silicon micromachined infrared sensor with tunable wavelength selectivity for application in infrared spectroscopy," *Sensors and Actuators A: Physical* **47**(1-3), 413–416 (1995). http://dx.doi.org/10.1016/0924-4247(94)00932-8.
10. Blomberg, M., Torkkeli, A., Lehto, A., Helenelund, C., and Viitasalo, M., "Electrically tuneable micromachined Fabry-Perot interferometer in gas analysis," *Physica Scripta* **T69**, 119–121 (1997). http://dx.doi.org/10.1088/0031-8949/1997/T69/018.
11. Vaughan, J. M., [*The Fabry-Perot Interferometer: History, Theory, Practice and Applications*], Hilger, Bristol (1989).
12. MacLeod, H. A., [*Thin-film Optical Filters*], Institute of Physics Pub., Bristol und Philadelphia (2001).
13. Hernandez, G., [*Fabry-Perot Interferometers*], Cambridge studies in modern optics, Cambridge Univ. Press, Cambridge (1988).
14. Jerman, J. H., Clift, D. J., and Mallinson, S. R., "A miniature Fabry-Perot interferometer with a corrugated silicon diaphragm support," *Sensors and Actuators A: Physical* **29**(2), 151–158 (1991). http://dx.doi.org/10.1016/0924-4247(91)87117-L.
15. Rossberg, D., *Untersuchung und Herstellung eines spektral-abstimmbaren Infrarot-Sensors in Silizium-Mikromechanik-Technologie für Anwendungen bei Zimmertemperatur*, PhD thesis, TU München, München (1996).
16. Rossberg, D., "Optical properties of the integrated infrared sensor," *Sensors and Actuators A: Physical* **54**(1-3), 793–797 (1996). http://dx.doi.org/10.1016/S0924-4247(97)80057-X.
17. Kanbara, N., Suzuki, K., Watanabe, T., and Iwaoka, H., "Precisely tunable Fabry-Perot filter for optical communications," in [*Conference Digest. 2002 IEEE/LEOS International Conference on Optical MEMS*], 173–174 (2002). http://dx.doi.org/10.1109/OMEMS.2002.1031498.
18. Atia, W., Flanders, D. C., Kotidis, P., and Kuznetsov, M. E., "US 7061618 B2: Integrated spectroscopy system," (2006).

19. Kotidis, P., Atia, W., Kuznetsov, M., Fawcett, S., Nislick, D., Crocombe, R., and Flanders, D. C., "Optical, tunable filter-based micro-instrumentation for industrial applications," *ISA Technical papers Collection* **439** (2003).
20. Flanders, D. C., Whitney, P. S., and Miller, F., "US 6341039 B1: Flexible membran for tunable Fabry-Perot filter," (2002).
21. Verghese, P. M., "US 7420738 B2: Dual membran single cavity fabry-perot MEMS filter," (2008).
22. Cook, C. C., "US 6618199 B2: Dual-band Farby-Pérot mirror coating," (2003).
23. Crocombe, R. A., Flanders, D. C., and Atia, W., "Micro-optical instrumentation for process spectroscopy," in [*Proc. SPIE 5591, Lab-on-a-Chip: Platforms, Devices, and Applications*], 11–25 (2004). http://dx.doi.org/10.1117/12.578107.
24. Neumann, N., Heinze, M., Stegbauer, H. J., Hiller, K., and Kurth, S., "Ein mikromechanisches, durchstimmbares Fabry-Perot-Filter für die nichtdispersive Gasanalytik im Spektralbereich 3...5 µm," in [*6. Dresdner Sensor Symposium*], (2003).
25. Neumann, N., Hiller, K., and Kurth, S., "Micromachined mid-infrared tunable Fabry-Perot filter," in [*13th Intern. Conf. on Solid-State Sensors, Actuators and Microsystems TRANSDUCERS'05*], 1010–1013 (2005). http://dx.doi.org/10.1109/SENSOR.2005.1496626.
26. Neumann, N., Ebermann, M., Kurth, S., and Hiller, K., "Tunable infrared detector with integrated micromachined Fabry-Perot filter," *Journal of Micro/Nanolithography, MEMS and MOEMS* **7**(2), 021004 1–9 (2008). http://dx.doi.org/10.1117/1.2909206.
27. Hiller, K., Kurth, S., Neumann, N., Heinz, S., and Geßner, T., "Comparison of low temperature bonding approaches for application in micro optical devices," in [*MikroSystemTechnik - KONGRESS 2007*], (2007).
28. Ebermann, M., Neumann, N., Hiller, K., Gittler, E., Meinig, M., and Kurth, S., "Widely tunable Fabry-Perot filter based MWIR and LWIR microspectrometers," in [*Proc. SPIE 8374, Next-Generation Spectroscopic Technologies V*], 83740X 1–9 (2012). http://dx.doi.org/10.1117/12.919169.
29. Schröter, J. R., Lehmann, S., Ebermann, M., and Neumann, N., "Wavelength stabilization of electrostatically actuated micromechanical infrared Fabry-Pérot filters," in [*Proc. SPIE 8868, Infrared Sensors, Devices, and Applications III*], 88680J 1–12 (2013). http://dx.doi.org/10.1117/12.2024822.
30. InfraTec GmbH, "FPI Detectors: Pyroelectric Detectors with Spectrometer Functionality," (2015). http://www.infratec-infrared.com/sensor-division/products/variable-color-detectors.html.
31. Ebermann, M., Neumann, N., Hiller, K., Gittler, E., Meinig, M., and Kurth, S., "Recent advances in expanding the spectral range of mems fabry-pérot filters," in [*Proc. SPIE 7594, MOEMS and Miniaturized Systems IX*], 75940V 1–10 (2010). http://dx.doi.org/10.1117/12.843441.
32. Ebermann, M., Neumann, N., Hiller, K., Seifert, M., Meinig, M., and Kurth, S., "Resolution and speed improvements of mid infrared fabry-perot microspectrometers for the analysis of hydrocarbon gases," in [*Proc. SPIE 8977, MOEMS and Miniaturized Systems XIII*], (2014). http://dx.doi.org/10.1117/12.2038235.
33. Ebermann, M., Neumann, N., Binder, S., Meinig, M., Seifert, M., Kurth, S., and Hiller, K., "A fast MEMS infrared microspectrometer for the measurement of hydrocarbon gases," in [*18th Intern. Conf. on Solid-State Sensors, Actuators and Microsystems (TRANSDUCERS)*], 2037–2040 (2015). http://dx.doi.org/10.1109/TRANSDUCERS.2015.7181356.
34. Meinig, M., Ebermann, M., Neumann, N., Kurth, S., Hiller, K., and Gessner, T., "Dual-band MEMS Fabry-Pérot filter with two movable reflectors for mid- and long-wave infrared microspectrometers," in [*16th Intern. Conf. on Solid-State Sensors, Actuators and Microsystems Transducers'11*], 2538–2541 (2011). http://dx.doi.org/10.1109/TRANSDUCERS.2011.5969764.
35. Meinig, M., Kurth, S., Helke, C., Seifert, M., Hiller, K., Ebermann, M., Neumann, N., and Gessner, T., "Electrically tunable Fabry-Pérot interferometer with inherent compensation of the influence of gravitation and vibration," in [*smart systems integration 2015*], (2015).
36. Kurth, S., Hiller, K., Neumann, N., Seifert, M., Ebermann, M., Zajadacz, J., Gessner, T., and Míguez, H. R., "Sub-wavelength structures for infrared filtering," in [*Proc. SPIE 7713, Photonic Crystal Materials and Devices IX*], 77131S 1–11 (2010). http://dx.doi.org/10.1117/12.854609.
37. Kurth, S., Hiller, K., Meinig, M., Besser, J., Seifert, M., Ebermann, M., Neumann, N., Schlachter, F., and Gessner, T., "Subwavelength grating reflectors in MEMS tunable Fabry-Perot infrared filters with large aperture," in [*Proc. SPIE 8995, High Contrast Metastructures III*], 89950I (2014). http://dx.doi.org/10.1117/12.2040339.

38. Rupprecht, J., Kurth, S., Hiller, K., Seifert, M., Besser, J., Meinig, M., Ebermann, M., Neumann, N., and Gessner, T., "Subwavelength Grating Reflectors for Fabrication Cost Reduction of Fabry-Perot Infrared Filters," *Materials Today: Proceedings* **2**(8), 4280–4288 (2015). http://dx.doi.org/10.1016/j.matpr.2015.09.014.
39. Gunning, W., Lauxtermann, S., Durmas, H., Xu, M., Stupar, P., Borwick, R., Cooper, D., Kobrin, P., Kangas, M., DeNatale, J., and Tennant, W., "MEMS-based tunable filters for compact IR spectral imaging," in [*Proc. SPIE 7298, Infrared Technology and Applications XXXV*], 72982I 1–9 (2009). http://dx.doi.org/10.1117/12.819017.
40. Gunning, W. J. and Southwell, W. H., "US 7319560 B2: Partitionated-cavity tynable Fabry-Pérot filter," (2008).
41. Gunning, W. J., DeNatale, J., Stupar, P., Borwick, R., Dannenberg, R., Sczupak, R., and Petterson, P. O., "Adaptive focal plane array: an example of MEMS, photonics, and electronics integration," in [*Proc. SPIE 5783, Infrared Technology and Applications XXXI*], 366–375 (2005). http://dx.doi.org/10.1117/12.606983.
42. Gunning, W. J., DeNatale, J., Stupar, P., Borwick, R., Lauxterman, S., Kobrin, P., and Auyeung, J., "Dual band adaptive focal plane array: an example of the challenge and potential of intelligent integrated microsystems," in [*Proc. SPIE 6232, Intelligent Integrated Microsystems*], 62320F 1–9 (2006). http://dx.doi.org/10.1117/12.669724.
43. Stupar, P. A., Borwick, R. L., DeNatale, J. F., Kobrin, P. H., and Gunning, W. J., "MEMS tunable Fabry-Perot Filters with thick, two sided optical coatings," in [*Solid-State Sensors, Actuators and Microsystems TRANSDUCERS*], 1357–1360 (2009). http://dx.doi.org/10.1109/SENSOR.2009.5285853.
44. Koskinen, Y., Letho, A., Tammela, S., Blomberg, M., Orpana, M., and Torkkeli, A., "US 5646729: Single-channel gas concentration measurement method and apparatus using a short-resonator Fabry-Perot interferometer," (1997).
45. Blomberg, M., Orpana, M., and Letho, A., "US 5561523: Electrically tunable Fabry-Perot interferometer produced by surface micromechanical techniques for use in optical material analysis," (1996).
46. Keränen, K., Blomberg, M., Tenhunen, J., and Karioja, P., "Analytic and raytrace modeling of a miniaturized infrared spectrometer module," in [*Technical Proceedings of the 2000 International Conference on Modeling and Simulation of Microsystems*], 660–663 (2000).
47. Keränen, K., Karioja, P., Rusanen, O., Tenhunen, J., Blomberg, M., and Lehto, H., "Electrically tunable nir spectrometer," in [*Proc. SPIE 3099, Micro-optical Technologies for Measurement, Sensors, and Microsystems II and Optical Fiber Sensor Technologies and Applications*], 181–184 (1997). http://dx.doi.org/10.1117/12.281225.
48. Koskinen, Y., "US 020120127482 A1: Method of controlling a short-etalon Fabry-Perot interferometer used in an ndir measurement apparatus," (2003).
49. Helenelund, C. P., "New type of CO2 sensor for ecological measurements," in [*26th Conference on Agricultural and Forest Meteorology*], (2004).
50. Saari, H., Mannila, R., Antila, J., Blomberg, M., Rusanen, O., Tenhunen, J., Wolf, L., and Harnisch, B., "Miniaturised gas sensor using a micromachined Fabry-Perot interferometer," in [*Proceedings of the Third Round Table on Micro/NanoTechnologies for Space*], **10**, 307–313 (2000).
51. Mannila, R., Tuohiniemi, M., Mäkynen, J., Näkki, I., and Antila, J., "Hydrocarbon gas detection with microelectromechanical Fabry-Perot interferometer," in [*Proc. SPIE 8726, Next-Generation Spectroscopic Technologies VI*], (2013). http://dx.doi.org/10.1117/12.2016362.
52. Mannila, R., Hyypiö, R., Korkalainen, M., Blomberg, M., Kattelus, H., and Rissanen, A., "Gas detection with microelectromechanical Fabry-Perot interferometer technology in cell phone," in [*Proc. SPIE 9482 Next-Generation Spectroscopic Technologies VIII*], 94820P (2015). http://dx.doi.org/10.1117/12.2176923.
53. Antila, J., Miranto, A., Mäkynen, J., Laamanen, M., Rissanen, A., Blomberg, M., Saari, H., and Malinen, J., "MEMS and piezo actuator-based Fabry-Perot interferometer technologies and applications at VTT," in [*Proc. SPIE 7680, Next-Generation Spectroscopic Technologies III*], 76800U 1–12 (2010). http://dx.doi.org/10.1117/12.850164.
54. Blomberg, M., Kattelus, H., and Miranto, A., "Electrically tunable surface micromachined Fabry–Perot interferometer for visible light," *Sensors and Actuators A: Physical* **162**(2), 184–188 (2010). http://dx.doi.org/10.1117/12.850164.

55. Rissanen, A., Akujärvi, A., Antila, J., Blomberg, M., and Saari, H., "MOEMS miniature spectrometers using tuneable Fabry-Perot interferometers," *Journal of Micro/Nanolithography, MEMS, and MOEMS* **11**(2), 023003–1 (2012). http://dx.doi.org/10.1117/1.JMM.11.2.023003.
56. Saari, H., "US 8130380 B2: Spectrometer and interferometric method," (2012).
57. Kantojärvi, U., Varpula, A., Antila, T., Holmlund, C., Mäkynen, J. H., Näsilä, A., Mannila, R., Rissanen, A., Antila, J. E., Disch, R. J., and Waldmann, T. A., "Compact large-aperture Fabry-Perot interferometer modules for gas spectroscopy at mid-IR," in [*Proc. SPIE 8992, Photonic Instrumentation Engineering*], 89920C (2014). http://dx.doi.org/10.1117/12.2036336.
58. Mannila, R., Näsilä, A., Viherkanto, K., Holmlund, C., Näkki, I., and Saari, H., "Spectral Imager based on Fabry-Perot interferometer for Aalto-1 nanosatellite," in [*Proc. SPIE 8870, Imaging Spectrometry XVIII*], 887002 (2013). http://dx.doi.org/10.1117/12.2023299.
59. Saari, H., Aallos, V.-V., Akujärvi, A., Antila, T., Holmlund, C., Kantojärvi, U., Mäkynen, J., and Ollila, J., "Novel miniaturized hyperspectral sensor for UAV and space applications," in [*Proc. SPIE 7474, Sensors, Systems, and Next-Generation Satellites XIII*], 74741M 1–12 (2009). http://dx.doi.org/10.1117/12.830284.
60. Antila, J., Mannila, R., Kantojärvi, U., Holmlund, C., Rissanen, A., Näkki, I., Ollila, J., and Saari, H., "Spectral imaging device based on a tuneable MEMS Fabry-Perot interferometer," in [*Proc. SPIE 8374, Next-Generation Spectroscopic Technologies V*], 83740F 1–10 (2012). http://dx.doi.org/10.1117/12.919271.
61. Rissanen, A., Mannila, R., and Antila, J., "Bragg reflectors for large optical aperture MEMS Fabry-Perot interferometers," in [*Proc. SPIE 8373, Micro- and Nanotechnology Sensors, Systems, and Applications IV*], 83732R 1–8 (2012). http://dx.doi.org/10.1117/12.920578.
62. Rissanen, A., Kantojärvi, U., Blomberg, M., Antila, J., and Eränen, S., "Monolithically integrated microspectrometer-on-chip based on tunable visible light MEMS FPI," *Sensors and Actuators A: Physical* **182**, 130–135 (2012). http://dx.doi.org/10.1016/j.sna.2012.05.023.
63. Rissanen, A., Mannila, R., Tuohiniemi, M., Akujärvi, A., and Antila, J., "Tunable MOEMS Fabry-Perot interferometer for miniaturized spectral sensing in near-infrared," in [*Proc. SPIE 8977, MOEMS and Miniaturized Systems XIII*], 89770X (2014). http://dx.doi.org/10.1117/12.2035732.
64. Tuohiniemi, M. and Blomberg, M., "Surface-micromachined silicon air-gap Bragg reflector for thermal infrared," *Journal of Micromechanics and Microengineering* **21**(7), 075014 1–7 (2011). http://dx.doi.org/10.1088/0960-1317/21/7/075014.
65. Tuohiniemi, M., Blomberg, M., Akujärvi, A., Antila, J., and Saari, H., "Optical transmission performance of a surface-micromachined Fabry–Pérot interferometer for thermal infrared," *Journal of Micromechanics and Microengineering* **22**(11), 115004 1–7 (2012). http://dx.doi.org/10.1088/0960-1317/22/11/115004.
66. Mäkynen, J. H., Tuohiniemi, M., Näsilä, A., Mannila, R., and Antila, J. E., "MEMS Fabry-Perot interferometer-based spectrometer demonstrator for 7.5 µm to 9.5 µm wavelength range," in [*Proc. SPIE 8977, MOEMS and Miniaturized Systems XIII*], 89770U (2014). http://dx.doi.org/10.1117/12.2036272.
67. Kantojärvi, U., Suhonen, J., and Antila, J., "MEMS spectral sensors bring laboratory measurements to field use," *Laser+Photonics* , 66–69 (2015).
68. Hamamatsu Photonics, "Mems-FPI spectrum sensor C13272: Mems-FPI tunable filter built-in compact NIR spectrum sensor," (2015). https://www.hamamatsu.com/us/en/community/optical_sensors/mems_devices/index.html.
69. Enomoto, T., Tanemura, T., Yamashita, S., Wado, H., Takeuchi, Y., and Hattori, Y., "Multi-Gas sensor by Infrared spectrometer," in [*Proceedings of the FISITA 2012 World Automotive Congress*], **194**, 611–620 (2012). http://dx.doi.org/10.1007/978-3-642-33829-8_57.
70. Suzuki, M., Wado, H., and Yoshida, T., "US 7733495 B2: Optical multilayer mirror and fabry-perot interferometer having the same," (2010).
71. Iwaki, T., Suzuki, M., Takeuchi, Y., and Tanemura, T., "US 020120127482 A1: Fabry-Perot interferometer," (2012).
72. Noro, M., Suzuki, K., Kishi, N., Hara, H., Watanabe, T., and Iwaoka, H., "CO2/H2O gas sensor using a tunable Fabry-Perot filter with wide wavelength range," in [*IEEE The Sixteenth Annual International Conference on Micro Electro Mechanical Systems, MEMS-03*], 319–322 (2003). http://dx.doi.org/10.1109/MEMSYS.2003.1189750.

73. Antoszewski, J., Dell, J. M., Shivakumar, T., Martyniuk, M., Winchester, K., Wehner, J., Musca, C. A., and Faraone, L., "Towards MEMS-based infrared tunable microspectrometers," in [*Proc. SPIE 4935, Smart Structures, Devices, and Systems*], 148–155 (2002). http://dx.doi.org/10.1117/12.476343.
74. Dell, J. M., Keating, A. J., Milne, J., Antoszewski, J., Musca, C. A., Faraone, L., Murphy, D., and Samardzic, O., "Micro-electromechanical systems-based microspectrometers covering wavelengths from 1500nm to 5000nm," in [*Proc. SPIE 6765, Next-Generation Spectroscopic Technologies*], 67650L 1–9 (2007). http://dx.doi.org/10.1117/12.732956.
75. Milne, J. S., Dell, J. M., Keating, A. J., and Faraone, L., "Widely tunable MEMS-based Fabry–Perot filter," *Journal of Microelectromechanical Systems* **18**(4), 905–913 (2009). http://dx.doi.org/10.1109/JMEMS.2009.2024793.
76. Tripathi, D. K., Mao, H., Silva, K. K. M. B. D., Bumgarner, J. W., Martyniuk, M., Dell, J. M., and Faraone, L., "Large-area mems-based distributed bragg reflectors for short-wave and mid-wave infrared hyperspectral imaging applications," *Journal of Microelectromechanical Systems* , 1 (2015). http://dx.doi.org/10.1109/JMEMS.2015.2477853.
77. Mao, H., Silva, K. K. M. B. D., Martyniuk, M., Antoszewski, J., Bumgarner, J., Nener, B. D., Dell, J. M., and Faraone, L., "MEMS-Based Tunable Fabry-Perot Filters for Adaptive Multispectral Thermal Imaging," *Journal of Microelectromechanical Systems* , 1–9 (2016). http://dx.doi.org/10.1109/JMEMS.2015.2509058.
78. Antoszewski, J., Winchester, K. J., Nguyen, T., Keating, A. J., Silva, D., Musca, C. A., Dell, J. M., Faraone, L., Silva, K. K. M. B. D., and Musca, C. A., "Materials and processes for MEMS-based infrared microspectrometer integrated on HgCdTe detector," *IEEE Journal of selected topics in quantum electronics* **14**(4), 1031–1041 (2008). http://dx.doi.org/10.1109/JSTQE.2008.919741.
79. Milne, J., Dell, J., Keating, A., Schuler, L., and Faraone, L., "Widely tunable Fabry-Perot optical filter using fixed-fixed beam actuators," in [*2008 IEEE/LEOS International Conference on Optical MEMs and Nanophotonics*], 66–67 (2008). http://dx.doi.org/10.1109/JSTQE.2008.919741.
80. Milne, J., Mittal, A., Dell, J., Keating, A., and Faraone, L., "Doubly-supported beam actuators for MEMS-based tunable Fabry-Perot etalons," in [*2006 Conference on Optoelectronic and Microelectronic Materials and Devices*], 220–223 (2006). http://dx.doi.org/10.1109/COMMAD.2006.4429920.
81. Antoszewski, J., Nguyen, T., Martyniuk, M., Dell, J. M., and Faraone, L., "Recent advances in SWIR MEMS-based tunable Fabry-Prot microspectrometers," in [*Proc. SPIE 8012, Infrared Technology and Applications XXXVII*], 80121X 1–6 (2011). http://dx.doi.org/10.1117/12.883734.
82. Tripathi, D. K., Silva, K. K. M. B. D., Bumgarner, J. W., Rafiei, R., Martyniuk, M., Dell, J. M., and Faraone, L., "Silicon-Air-Silicon Distributed Bragg Reflectors for Visible and Near Infrared Optical MEMS," *Journal of Microelectromechanical Systems* **24**(5), 1245–1247 (2015). http://dx.doi.org/10.1109/JMEMS.2015.2459076.
83. Sabaté, N., Rubio, R., Calaza, C., Santander, J., Fonseca, L., Gràcia, I., Cané, C., Moreno, M., and Marco, S., "Mirror electrostatic actuation of a medium-infrared tuneable Fabry-Perot interferometer based on a surface micromachining process," *Sensors and Actuators A: Physical* **123-124**, 584–589 (2005). http://dx.doi.org/10.1016/j.sna.2005.03.036.
84. Calaza, C., Meca, E., Marco, S., Moreno, M., Samitier, J., Fonseca, L., Gracia, I., and Cane, C., "Assessment of the final metrological characteristics of a MOEMS-based NDIR spectrometer through system modeling and data processing," *IEEE Sensors Journal* **3**(5), 587–594 (2003). http://dx.doi.org/10.1109/JSEN.2003.817672.
85. Calaza, C., Fonseca, L., Moreno, M., Marco, S., Cané, C., and Gracia, I., "A surface micromachining process for the development of a medium-infrared tuneable Fabry–Perot interferometer," *Sensors and Actuators A: Physical* **113**(1), 39–47 (2004). http://dx.doi.org/10.1016/j.sna.2004.01.047.